



Contents lists available at ScienceDirect

Bioorganic & Medicinal Chemistry

journal homepage: www.elsevier.com/locate/bmc

Novel naphtho[2,1-*d*]oxazole-4,5-diones as NQO1 substrates with improved aqueous solubility: Design, synthesis, and in vivo antitumor evaluation

Xiang Li^{a,b,†}, Jinlei Bian^{a,†}, Nan Wang^a, Xue Qian^a, Jing Gu^a, Tong Mu^a, Jun Fan^a, Xiuwen Yang^a, Shangzhen Li^a, Tingting Yang^a, Haopeng Sun^{a,c}, Qidong You^{a,*}, Xiaojin Zhang^{a,c,*}

^a Jiangsu Key Laboratory of Drug Design and Optimization, and State Key Laboratory of Natural Medicines, China Pharmaceutical University, Nanjing 210009, China

^b Department of Pharmaceutical Engineering, China Pharmaceutical University, Nanjing 210009, China

^c Department of Organic Chemistry, China Pharmaceutical University, Nanjing 210009, China

ARTICLE INFO

Article history:

Received 24 November 2015

Revised 13 January 2016

Accepted 14 January 2016

Available online xxx

Keywords:

NQO1 substrates

β-Lapachone

Antitumor

ortho-Naphthoquinones

In vivo

ABSTRACT

A new series of *ortho*-naphthoquinone analogs of β-lapachone were designed, synthesized and evaluated. The biological results indicated that most of our compounds were efficient substrates for NQO1. The new scaffold with water-soluble side chain resulted in greater solubility under acidic condition compared to β-lapachone. Thus avoiding the use of hydroxylpropyl β-cyclodextrin which would finally cause the rapid drug clearance from the blood and dose-limiting toxicity in the form of hemolytic anemia. The most soluble and promising compound in this series was 2-((4-benzylpiperazin-1-yl)methyl)naphtho[2,1-*d*]oxazole-4,5-dione (**3k**), which inhibited cancer cell (NQO1-rich A549 cell line) growth at IC₅₀ values of 4.6 ± 1.0 μmol·L⁻¹. Furthermore, compound **3k** had in vivo antitumor activity in an A549 tumor xenografts mouse model comparable to the activity obtained with β-lapachone. The results indicated that these *ortho*-naphthoquinones could serve as promising leads for further optimization as novel substrates for NQO1.

© 2016 Elsevier Ltd. All rights reserved.

1. Introduction

NAD(P)H:quinone oxidoreductase-1 (NQO1) is a homodimeric flavoprotein that catalyzes the obligatory two-electron reduction of quinones to hydroquinones using NADH or NADPH as cofactor.^{1,2} Typically, this reduction detoxifies quinones, forming less reactive hydroquinones. Glutathione S-transferase then detoxifies hydroquinones, conjugating them with glutathione for secretion.³ While the two-electron reduction process has made some compounds biologically active. Moreover, the reduced hydroquinones may be oxidized back to quinones followed by subsequent generation of reactive oxygen species (ROS) and oxidative stress.⁴ The accumulated ROS via redox cycling can achieve selectivity toward cancer cells due to the high basal redox levels uniquely present in it.^{5,6}

Overexpression of NQO1 in cancer cells further makes it be a promising therapeutic target for tumor-selective drug therapy with reduced toxicities to normal cells that express little to no

levels of the enzyme.^{7,8} Recently, several *ortho*-naphthoquinones have been reported to be efficient substrates for NQO1.^{9–11} For example, β-lapachone (β-lap), a natural *ortho*-naphthoquinone isolated from the Bignoniaceae family and is currently in multiple phase II clinical trials.^{12–14} While capable of killing cancer cells, β-lap demonstrated limited water solubility. In the clinical studies, the use of hydroxylpropyl β-cyclodextrin (HPβCD) (ARQ501 and ARQ761) to formulate β-lap showed a 400-fold increase in solubility.¹⁵ However, rapid drug clearance from the blood and dose-limiting toxicity in the form of hemolytic anemia due to HPβCD were observed. These are the reasons why the clinical form of ARQ501 and ARQ761 underwent unsuccessful clinical trials in patients with several different cancers.¹⁶ Lately, we reported an efficient NQO1 substrate (**DDO-7101, 2**),¹⁰ which possessed better specificity and safety than β-lap. Despite the potency and selectivity of **2** in killing NQO1-containing cancer cells in vitro, demonstrated even lower water solubility of **2** (0.021 mg/ml) than β-lap (0.043 mg/ml) which is limited back in its application in vivo. Therefore, for in vivo evaluation studies, it was necessary to improve the solubility of **2** (see Fig. 1).

Herein, as part of our ongoing program, we reported a series of new scaffold of naphtho[2,1-*d*]oxazole-4,5-diones (**3**) with

* Corresponding authors.

E-mail addresses: youqd@163.com (Q. You), zxj@cpu.edu.cn (X. Zhang).

† These two authors contributed equally to this work.

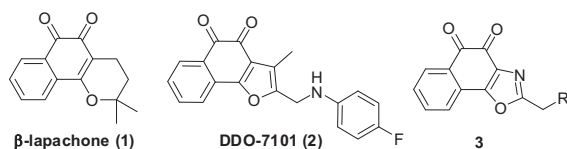


Figure 1. The structures of β -lapachone, DDO-7101 and the new designed structure 3.

improved aqueous solubility, as novel efficient NQO1 substrates. These *ortho*-naphthoquinones have been tested in vitro for their antitumor activity against NQO1-rich cancer cell lines. Compound **3k**, which was the most potent and drug-like, was further investigated on the mechanism demonstrated that this compound was selective toxic towards cancer cell line with high NQO1 activity and had a capability to induce ROS. It was remarkably suppressed tumor in the in vivo A549 tumor xenografts mouse model, which was comparable to the activity obtained with β -lap. Thus, the compound was deserved further optimization with the aim to obtain antitumor agents through NQO1-dependent and ROS-mediated pathways.

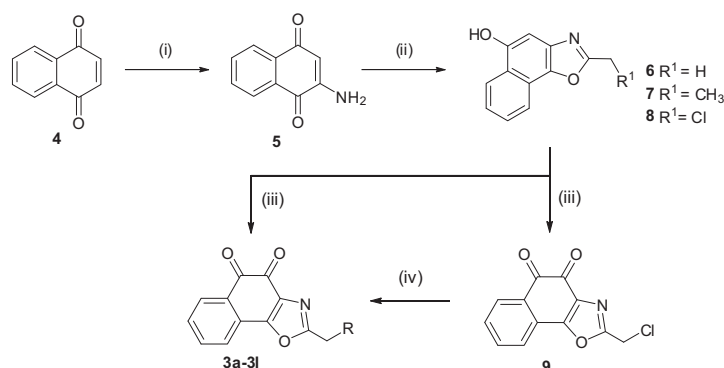
2. Results and discussion

2.1. Chemistry

The designed 12 *ortho*-naphthoquinone target compounds **3a–3l** were synthesized according to the protocol outlined in Scheme 1. The reaction of **4** with sodium azide at room temperature provided the product **5** in a yield of 83%. Treatment of **5** with substituted aldehydes gave rise to 2-substituted 5-hydroxynaphtho[2,1-*d*]oxazoles **6–8** in moderate yields (Scheme 1). Generally, these hydroxynaphtho[2,1-*d*]oxazoles could be simply concentrated in oil pump vacuum to remove traces of the aldehyde reactants, leaving the products in purities of more than 95%. Oxidation of **6–8** using the reagent Fremy's salt provided the target compounds **9**, **3a** and **3b** in 72–85% yield. The other target compounds **3c–3l** that substituted with amine side chains were synthesized by a nucleophilic substitution with corresponding amines. All of the compounds were confirmed by ^1H NMR, IR and EI spectrum. The representative compounds **3a**, **3d**, **3g**, **3k** and **3l** were further confirmed by ^{13}C NMR.

2.2. Enzyme studies

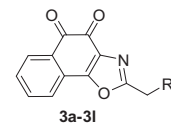
All of the *ortho*-naphthoquinone derivatives were evaluated for their ability to act as substrates for NQO1. The ability of NQO1 to process the naphthoquinones in vitro at the concentration of



Scheme 1. Reagents and conditions: (i) Sodium azide, THF/HCl, HOAc, rt, 7 h; (ii) R¹CH₂CHO, HBr, HAc, rt, 12–16 h; (iii) Fremy's salt, 0 °C–rt, 1–3 h; (iv) DMF, KI, K₂CO₃, 45 °C, 1–5 h. For the detailed R groups of compounds **3a–3l**, see Table 1.

Table 1

Metabolism by NQO1 of *ortho*-naphthoquinones monitored by enzyme labeling instrument at the absorbance of A₃₄₀ nm and cytotoxicity toward A₅₄₉ (NQO1-rich) cell lines



Entry	R	Metabolism by NQO1 ($\mu\text{mol NADPH}/\text{min}/\mu\text{mol NQO1}$)	Cytotoxicity IC ₅₀ ($\mu\text{mol}\cdot\text{L}^{-1}$)
3a	H	1202 ± 87	20 ± 4.3
3b	Me	955 ± 44	7.6 ± 0.6
3c	Me ₂ N	939 ± 78	8.7 ± 2.0
3d	Morpholino	686 ± 52	6.9 ± 1.8
3e	<i>o</i> -MeO-PhNH	990 ± 37	11 ± 0.5
3f	<i>m</i> -MeO-PhNH	955 ± 38	15 ± 4.9
3g	<i>p</i> -MeO-PhNH	1063 ± 45	13 ± 2.8
3h	<i>p</i> -Me-PhNH	968 ± 76	12 ± 1.5
3i	<i>p</i> -Cl-PhNH	1522 ± 121	19 ± 9.3
3j	<i>m</i> -F-PhNH	1391 ± 78	5.2 ± 0.1
3k	4-Benzylpiperazin-1-yl	1360 ± 30	4.6 ± 1.0
3l	4-Phenylpiperazin-1-yl	1139 ± 42	7.6 ± 1.3
β -lap	–	1210 ± 30	3.7 ± 0.5

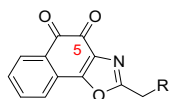
10 $\mu\text{mol}\cdot\text{L}^{-1}$ was assessed. The quinone substrates were coincubated with both human NQO1 as well as NADPH. It was capable of quantifying NADPH oxidation to NADP⁺ by monitoring the absorbance (A₃₄₀ nm) on an enzyme labeling instrument.¹⁷ As previously reported, the results of the quinone reduction were presented as $\mu\text{mol}\cdot\text{L}^{-1}$ NADPH oxidized $\text{min}^{-1}\cdot\mu\text{mol}^{-1}$ NQO1.

In general, most of the *ortho*-naphthoquinones (**3a–3l**) possessed moderate to good reduction rates by NQO1, indicating that these compounds were good substrates for NQO1 (Table 1). Among them, compounds **3i** and **3j** with halogen substitution at the benzene moiety exhibited higher enzymatic conversion rates (1391–1522 $\mu\text{mol NADPH}/\text{min}/\mu\text{mol NQO1}$) than other compounds. Notably, compounds **3k** and **3l** with aromatic piperazinyl, which is designed for the purpose of improving their drug-like properties, showed efficient reduction rate by NQO1 (1139–1360 $\mu\text{mol NADPH}/\text{min}/\mu\text{mol NQO1}$). In short, compounds **3i–3l** exhibited comparable enzymatic conversion rate (1139–1522 $\mu\text{mol NADPH}/\text{min}/\mu\text{mol NQO1}$) compared to β -lap and thus them ranked as the efficient substrates for NQO1.

2.3. Molecular docking

To elucidate the possible binding mode of NQO1 with the naphthoquinones, molecular docking of the representative compounds

Table 2
ChemScore and reduction rates of the representative compounds



Compound	ChemScore	C=O5...NH5 (Å)	Metabolism by NQO1 (μmol NADPH/min/μmol NQO1)
3a	75.71	3.75	1202 ± 87
3i	95.45	3.80	1522 ± 121
3k	91.75	3.82	1360 ± 30
β-lap	69.43	3.31	1210 ± 30

3a, **3i**, **3k** and the control compound β-lap with NQO1 were performed on the binding model based on the NQO1 complex structure (PDB code 2F10) using Gold 5.1.^{18,19} ChemScore function was explored during the docking experiments (Table 2). Higher score represented better fit for the model. Of the selected compounds studied, compound **3i** was nicely bound into the active site of NQO1 with highest score. The ChemScore values of these compounds had the same trend as their reduction rates by NQO1, which likely to prove the correlation between the reduction rates and the binding affinity.

The binding model of the selected compounds with NQO1 complex was carefully analyzed and the results were shown in Figure 2. All of the *ortho*-naphthoquinones including β-lap oriented with quinone ring above the isoalloxazine ring of the bound cofactor FAD as for hydride transfer by π-stacking interaction, which were similar to the crystal structures of substrates or inhibitors in complex with NQO1.^{20,21} Similar to our previously reported compounds,^{10,11} the two carbonyl groups in the *ortho*-naphthoquinone substrates and β-lap could bind firmly to the Tyr126 and Tyr128 residues by hydrogen bonding interactions. For compounds **3a**, **3i** and **3k**, compared to the control β-lap, the nitrogen atom in the

oxazole ring could form another hydrogen bond with Tyr128, providing a rationale for the better activity of these series of quinone with oxazole scaffold. There existed an additional pocket formed by Tyr128, Met154, Phe232, Phe236 and His194 for side chains occupying. As depicted in Figure 2, for L-shaped compounds **3i** and **3k**, the substituted amine side chains can occupy the additional pocket, explained the better activity of the L-shaped compounds compared to compounds without the side chains. Besides, forming π-stacking interactions with Tyr128 in the active site of NQO1, explained the fact that the aromatic amine analogs exhibited higher reduction rates by NQO1 than other compounds. As for compound **3k**, with larger side chain, which did not substantially decrease the reduction rate compared to **3i**. This result indicated that the side pocket is sufficiently flexible so as to accommodate variety of side chains. Moreover, the C–H...π interaction formed by piperazinyl with the Tyr128 and the benzyl in the side chain with adjacent Phe232 residue, further explained the reason for the considerable activity of compound **3i**.

In addition, our recent molecular modeling studies have demonstrated that the quinone substrates to be metabolized by NQO1 required an appropriate hydride donor–acceptor distance between the substrate (quinone carbonyl) and the FAD cofactor (atom N5 which transfer the hydride).²² As illustrated in Figure 2, all were within a reasonable distance (about 4 Å) for hydride transfer from the reduced FAD (FADH₂) to quinone substrates.

2.4. Physicochemical properties

To verify our hypothesis that this series of compounds were obtained with improved solubility and in an effort to identify potential drug-like compounds prior to the time-consuming and costly development to optimize derivatives that may ultimately fail in *in vivo* efficacy experiments, then the representative compounds with efficient enzymatic conversion rates were selected to determine their solubility and Log_{D7.4} (Table 3). Two methods were employed to determine the solubility. Their intrinsic aqueous

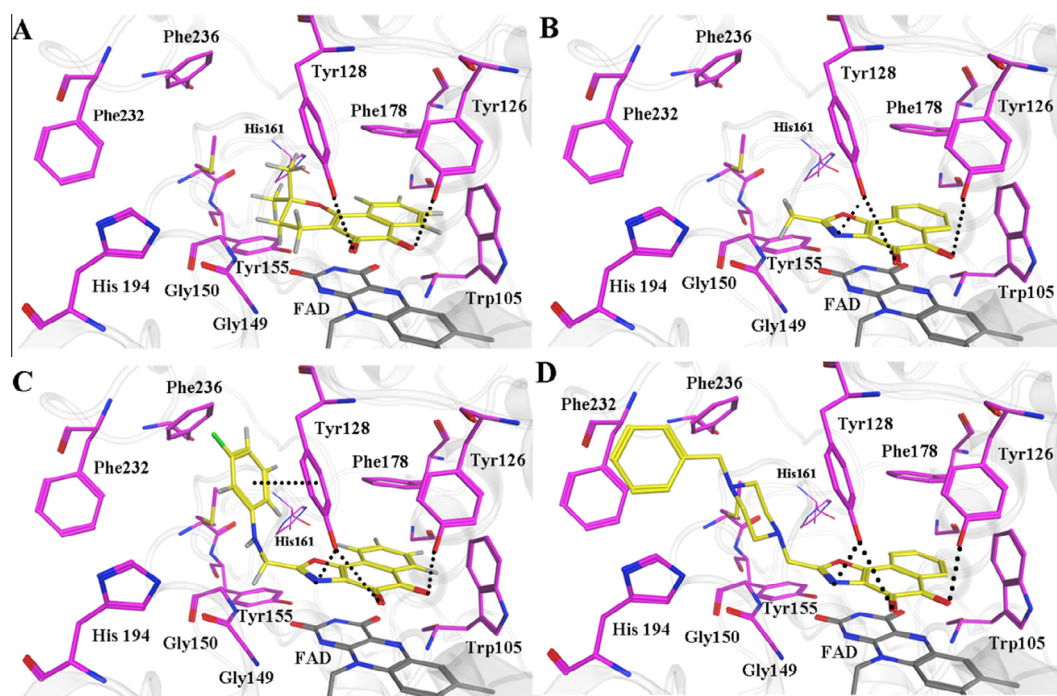


Figure 2. Docked conformation of compounds β-lap (A), **3a** (B), **3i** (C) and **3k** (D) into active site of NQO1. The interaction mode was obtained through molecular docking (PDB id: 2F10) and depicted using MOE 2013.08. The carbon atoms of the compounds and the key residues in the active site of NQO1 were colored in yellow and purple, respectively. The H-bonds were shown as black dot lines.

Table 3
Physicochemical properties of the selected compounds

Compound	Intrinsic solubility (µg/mL)	Solubility ^a (pH = 3) (µg/mL)	LogD (pH 7.4)
3i	38	<100	2.65
3j	44	<100	3.18
3k	125	>500	1.88
β-lap	43	<100	2.85

^a Determined in diluted hydrochloric acid buffer at pH = 3.

solubility was determined on a Gemini Profiler instrument (pION) by the 'goldstandard' Avdeef–Bucher potentiometric titration method. For their intrinsic aqueous solubility, except for **3k** with three times more soluble (125 µg/mL) than β-lap, other compounds were on the same level with it. The other method was used to determine their solubility under acidic condition, most of these compounds (**3c–3h**, **3k–3l**) (data not shown) showed dramatically increased solubility (solubility of >100 µg/mL in diluted hydrochloric acid buffer at pH = 3). The hydrophobicity parameters LogD_{7.4} are also summarized in Table 3. These compounds also showed acceptable LogD_{7.4} values. Thus, compound **3k** showed the best physicochemical properties among the selected compounds (LogD_{7.4} 1.88, intrinsic solubility 125 µg/mL and solubility under acidic condition >500 µg/mL) and could be selected for further pharmacological both in vitro and in vivo.

2.5. Cytotoxicity evaluation

Cytotoxicity studies were performed on the *ortho*-naphthoquinones with cell survival being determined by the MTT assay against the human non-small cell lung cancer A549 cell line (NQO1-rich). β-Lap was used as positive control. The results of cytotoxic activity in vitro were expressed as the IC₅₀ (Table 1).

As shown in Table 1, it was found that all the compounds showed moderate to potent cytotoxicity against A549 cancer cell line (NQO1-rich) with IC₅₀ values ranging from 4.6 to 20 µmol·L⁻¹. Most of the analogs possessed comparative cytotoxicity to the positive control β-lap against A549 cancer cell line. Taken together of the physicochemical properties and activity, the most potent and drug-like compound **3k** was further tested against H596 (NQO1-deficient), L02 (normal hepatic cell lines) and A549 cell lines in the presence of the NQO1 inhibitor dicoumarol (DIC, 25 µmol·L⁻¹) to compare the cytotoxicity. Coincubation with DIC greatly protected A549 cells from the cell death mediated by **3k**, shifting the IC₅₀ > 7-fold. (The fold is the ratio of the IC₅₀ of cotreatment with quinone and DIC to the IC₅₀ of treatment with only quinone, and a higher ratio indicates greater protection and greater NQO1

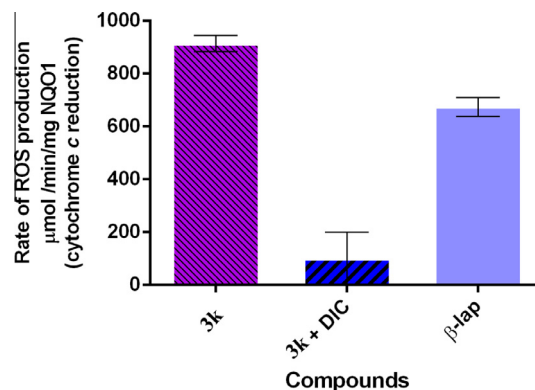


Figure 4. Rate of ROS production of **3k** in the presence and absence of the NQO1 inhibitor (DIC, 25 µmol·L⁻¹) with NQO1 and rates are expressed as mean ± SD, $P < 0.001$ versus control ($n = 3$). (Spectrophotometric assay with cytochrome *c* as terminal electron acceptor (550 nm).)

specificity) (Fig. 3). Meanwhile, compound **3k** showed much less toxic against H596 lung cancer cell line (NQO1-deficient), shifting the IC₅₀ > 12-fold. These results revealed that the efficient NQO1 substrate **3k** was selective towards cancer cell line with high NQO1 activity. In addition, **3k** was further evaluated for its toxicity towards the human normal hepatic cell line L02, a superior safety profile was confirmed. Because of the excellent antitumor activity, selective toxic towards cancer cell lines and good solubility, **3k** was selected for further detailed analysis.

2.6. Determination of ROS production

Compound **3k** was selected as the representative compound to investigate the ability of producing ROS. We investigated whether the compound was able to generate ROS in the direct interaction of NQO1. The production of the superoxide was measured by a spectrophotometric assay with cytochrome *c* as the terminal electron acceptor.²³ The initial rates (µmol cytochrome *c* reduced/min/mg NQO1) were calculated from the linear portion (0–30 s) of the reduction graphs. **3k** showed slightly higher rates of ROS compared to β-lap, and coincubation with dicoumarol (DIC) dramatically reduced the rate of ROS production (Fig. 4). The result indicated that compound **3k** could generate a high amount of ROS through NQO1-directed redox cycling.

2.7. In vivo antitumor activity

Having obtained the excellent soluble and cytotoxic properties of **3k** in in vitro studies, we further evaluated the in vivo antitumor efficacy of the compound in A549 tumor xenografts mouse model (Fig. 5). Nude mice bearing established A549 tumor xenografts were injection with compound **3k** (15 mg/kg or 30 mg/kg daily over a 21-day period). β-Lap (ARQ501, 30 mg/kg) was used as a positive control drug. Tumor growth inhibition (TGI) and relative tumor proliferation rate (*T/C*) were calculated to reveal the antitumor effects in tumor weight and tumor volume, respectively. Compared to the vehicle-treated control group, both of the 15 mg/kg and 30 mg/kg showed significant in vivo antitumor efficacy (Fig. 5A) and produced no evident toxic signs in liver. Compound **3k** (30 mg/kg) demonstrated potent in vivo antitumor activity with comparable TGI value (55.6%) and *T/C* value (41.4%) to β-lap (TGI = 70.1%, *T/C* = 29.5%) (Fig. 5A and B). Consistent with these results, the volume of tumors (440.8 ± 105.9 mm³) was obviously decreased when treated with **3k** (30 mg/kg) compared with the control group (1085.8 ± 298.3 mm³) (Fig. 5C). Besides, in the mice group treated by **3k**, no significant body weight loss

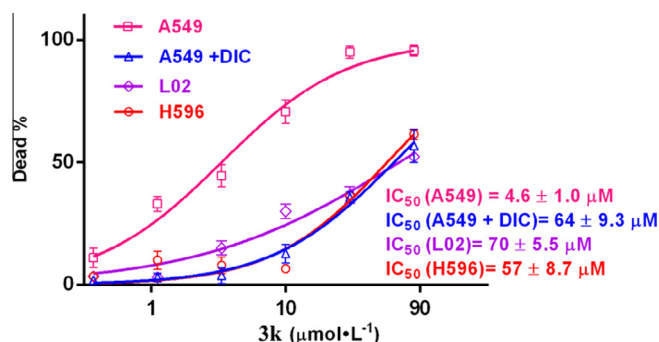


Figure 3. Cell death of A549 cells treated with compound **3k** in the presence and absence of the NQO1 inhibitor (DIC, 25 µmol·L⁻¹). H596 (NQO1-deficient) and L02 (normal hepatic cell lines) were evaluated to compare the cytotoxicity with A549 cell lines (NQO1-rich cancer cell).

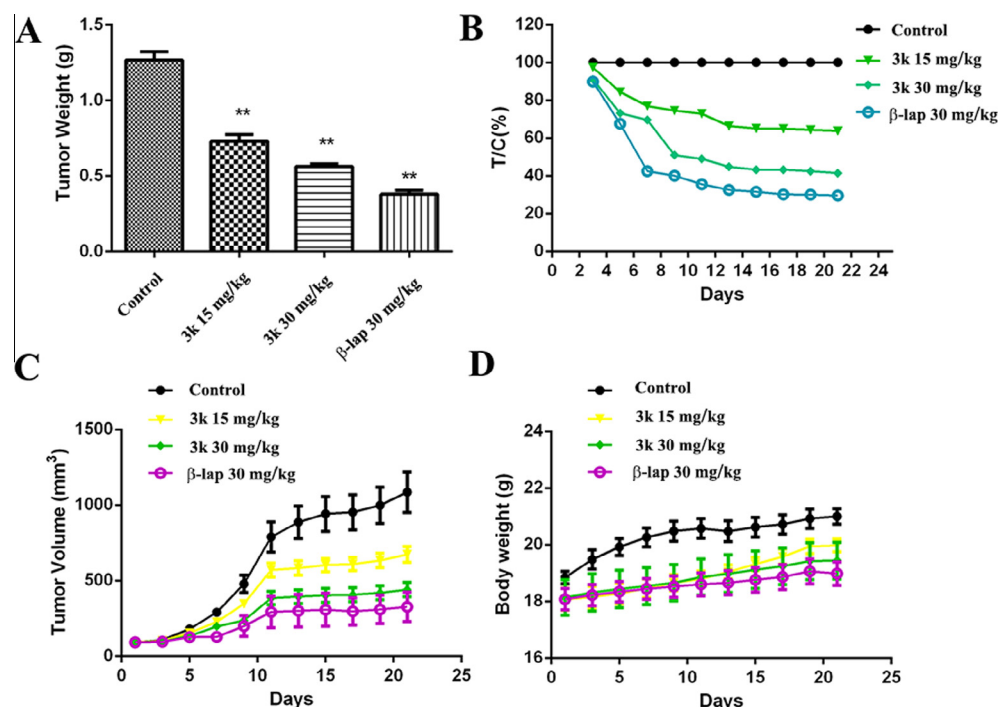


Figure 5. Compound **3k** retards the tumor growth in vivo in A549 tumor xenografted nude. (A) Tumor weight measurement ($^{**}p < 0.01$). (B) Relative tumor proliferation rate (T/C) measurement. $T/C (\%) = T_{RTV}/C_{RTV} \times 100$; $RTV = V_t/V_0$; T_{RTV} represents the test group; C_{RTV} represents the control group. (C) Tumor volume measurement. (D) Body weight measurement.

was observed comparison with the vehicle control group (Fig. 5D). Thus, our studies suggest that compound **3k** would be promising anticancer therapeutic for the treatment of cancer.

3. Conclusions

As an alternative to the previously described *ortho*-quinone substrates for NQO1, we described herein the design, synthesis and evaluation of 12 naphtho[2,1-*d*]oxazole-4,5-diones as anticancer agents. These *ortho*-naphthoquinones were characterized and evaluated as efficient substrates for NQO1. This series of compounds showed moderate to good solubility under acidic condition. Determination of ROS production and in vitro cytotoxicity evaluation in the presence of the NQO1 inhibitor DIC confirmed that these compounds exerted their antitumor activity through NQO1-mediated ROS production via redox cycling. Moreover, highlighting compound **3k** (named as **DDO-7132**) exhibited comparable anticancer activity and superior safety profile as compared to β -lap both in vitro and in vivo, which might be a promising and novel candidate. Supported by these investigations, current efforts in our group are focus on generation of novel *ortho*-quinone analogs with enhanced and potent antitumor activity.

4. Experimental

4.1. Chemistry

All reagents were purchased from commercial sources. Organic solutions were concentrated in a rotary evaporator (BüchiRotavapor) below 55 °C under reduced pressure. Reactions were monitored by thin-layer chromatography (TLC) on 0.25 mm silica gel plates (GF254) and visualized under UV light. Melting points were determined with a Melt-Temp II apparatus. The ^1H NMR and ^{13}C NMR spectra were measured on a Bruker AV-300 instrument using deuterated solvents with tetramethylsilane (TMS) as internal

standard. IR spectra were recorded on a Nicolet iS10 Avatar FT-IR spectrometer using KBr film. EI-MS was collected on Shimadzu GCMS-2010 instruments. ESI-mass and high resolution mass spectra (HRMS) were recorded on a Water Q-ToFmicro mass spectrometer. Analytical results are within 0.40% of the theoretical values.

4.1.1. 2-Amino-1,4-naphthoquinone (5)

6.25 g NaN_3 was dissolved in 15 mL H_2O and acidified with 5 mL glacial acetic acid. The NaN_3 solution was added to a solution of 1,4-naphthoquinone (5 g, 29 mmol) dissolved in 100 mL of THF/ H_2O (4:1) and stirred at room temperature. After 8 h, the reaction was poured into cold water and then the precipitate was obtained. The reddish brown residue was recrystallized from ethanol to yield 4.0 g **5** (80% yield). Mp 105–106 °C, ^1H NMR (300 MHz, DMSO) δ : 7.95–7.70 (m, 4H), 7.24 (s, 2H), 5.82 (s, 1H), EI-MS: 173.

4.1.2. 2-Methyl-5-hydroxynaphtho[2,1-*d*]oxazole (6)

2-Amino-1,4-naphthoquinone **5** (500 mg, 2.8 mmol) was dissolved in acetic acid (10 mL), after which a 33% solution of HBr in acetic acid (0.5 mL) and the aldehyde (14.0 mmol) were added dropwise. The reaction mixture was stirred at room temperature for 6–12 h. After completion the reaction mixture was diluted with water and extracted with diethyl ether. The combined organic extracts were washed with aqueous sodium bicarbonate, aqueous sodium sulfite and brine. Drying over MgSO_4 , followed by filtration and concentration in vacuo gave the crude product. The product was ready for the next step without the further purification.

4.1.3. 2-Ethyl-5-hydroxynaphtho[2,1-*d*]oxazole (7)

2-Amino-1,4-naphthoquinone **5** (500 mg, 2.8 mmol) was dissolved in acetic acid (10 mL), after which a 33% solution of HBr in acetic acid (0.5 mL) and the propionaldehyde (14.0 mmol) were added dropwise. The reaction mixture was stirred at room temperature for 6 h. After completion the reaction mixture was diluted with water and extracted with diethyl ether. The combined organic

extracts were washed with aqueous sodium bicarbonate, aqueous sodium sulfite and brine. Drying over MgSO_4 , followed by filtration and concentration in vacuo gave the crude product. The product was ready for the next step without the further purification.

4.1.4. 2-Chloromethyl-5-hydroxynaphtho[2,1-d]oxazole (8)

2-Amino-1,4-naphthoquinone **5** (5 g, 28 mmol) was dissolved in acetic acid (20 mL), after which a 33% solution of HBr in acetic acid (3 mL) and the chloroacetaldehyde (140 mmol) were added dropwise. The reaction mixture was stirred at room temperature for 12 h. After completion the reaction mixture was diluted with water and extracted with diethyl ether. The combined organic extracts were washed with aqueous sodium bicarbonate, aqueous sodium sulfite and brine. Drying over MgSO_4 , followed by filtration and concentration in vacuo gave the crude product. The product was ready for the next step without the further purification.

4.1.5. General procedure for the preparation of compounds **3a**, **3b** and **9**

To a solution of naphthol (**6–8**, 1 mmol) in acetone (10 mL) was added a solution of Fremy's salt in KH_2PO_4 buffer (0.65 mol·L⁻¹, 30 mL). The reaction mixture was stirred at room temperature for 2–6 h. After that, the acetone was evaporated under reduced pressure, giving a red precipitate. The precipitate was then collected and purified by recrystallization from ethanol to give the products (**3a**, **3b** and **9**).

4.1.5.1. 2-Methylnaphtho[2,1-d]oxazole-4,5-dione (3a). Yield: 82%. Red solid, mp 180–181 °C. ¹H NMR (300 MHz, CDCl_3) δ : 8.17 (d, J = 7.5 Hz, 1H), 7.72–7.70 (m, 2H), 7.60–7.54 (m, 1H), 2.67 (s, 3H). ¹³C NMR (75 MHz, CDCl_3) δ : 179.8, 175.1, 161.6, 139.3, 137.5, 127.3, 124.2, 123.6, 122.7, 119.8, 119.3, 11.7. IR (ν , cm^{-1}): 3415, 2361, 1683, 1638, 1592, 1561, 1228, 1065, 1002, 839, 581. ESI-HRMS m/z [$\text{M}+\text{Na}$]⁺ calculated for $\text{C}_{12}\text{H}_7\text{NO}_3\text{Na}$: 236.0318, found: 236.0312.

4.1.5.2. 2-Ethynaphtho[2,1-d]oxazole-4,5-dione (3b). Yield: 70%. Dark red solid, mp 190–192 °C. δ : 8.09 (d, J = 7.8 Hz, 1H), 7.63 (d, J = 3.8 Hz, 2H), 7.50–7.45 (m, 1H), 2.90 (q, J = 7.6 Hz, 2H), 1.39 (t, J = 7.6 Hz, 3H). IR (ν , cm^{-1}): 3415, 1265, 1562, 1229, 1067, 838, 573. ESI-HRMS m/z [$\text{M}+\text{Na}$]⁺ calculated for $\text{C}_{13}\text{H}_9\text{NO}_3\text{Na}$: 250.0475, found: 250.0470.

4.1.5.3. 2-Chloromethylnaphtho[2,1-d]oxazole-4,5-dione (9). Yield: 75%. Red solid, mp 175–177 °C. ¹H NMR (300 MHz, DMSO) δ : 8.02 (d, J = 7.4 Hz, 1H), 7.78 (s, 2H), 7.68–7.63 (m, 1H), 5.10 (s, 2H). IR (ν , cm^{-1}): 3414, 3041, 2985, 2360, 2341, 1683, 1641, 1402, 1244, 1213, 1050, 781. ESI-HRMS m/z [$\text{M}+\text{Na}$]⁺ calculated for $\text{C}_{12}\text{H}_6\text{ClNO}_3\text{Na}$: 269.9928, found: 269.9931.

4.1.6. General procedure for the preparation of compounds **3c–3l**

To a mixture of amine (0.48 mmol), KI (10 mg, 0.06 mmol), K_2CO_3 (55 mg, 0.40 mmol) in DMF (5 mL) was added naphthoquinone **9** (100 mg, 0.40 mmol). The resulting mixture was stirred at 55 °C for 1–2 h. After being cooled, the mixture was poured into ice water and the resulting mixture was extracted with EtOAc. The combined organic layer was washed with brine and dried over anhydrous Na_2SO_4 , filtered and concentrated to afford a crude product, which was purified through column chromatography over silica gel.

4.1.6.1. 2-((Dimethylamino)methyl)naphtho[2,1-d]oxazole-4,5-dione (3c). Yield: 75%. Red solid, mp 162–164 °C. ¹H NMR (300 MHz, CDCl_3) δ : 8.17 (d, J = 7.5 Hz, 1H), 7.80–7.72 (m, 2H),

7.58 (t, J = 7.8 Hz, 1H), 3.83 (s, 2H), 2.45 (s, 6H). IR (ν , cm^{-1}): 3476, 3414, 2962, 1678, 1585, 1219, 1048, 911, 473. ESI-HRMS m/z [$\text{M}+\text{NH}_4$]⁺ calculated for $\text{C}_{14}\text{H}_{16}\text{N}_3\text{O}_3$: 274.1186, found: 274.2744.

4.1.6.2. 2-((Morpholino)methyl)naphtho[2,1-d]oxazole-4,5-dione (3d). Yield: 53%. Red solid, mp 170–172 °C. ¹H NMR (300 MHz, CDCl_3) δ : 8.15 (d, J = 7.4 Hz, 1H), 7.77–7.69 (m, 2H), 7.57 (t, J = 7.1 Hz, 1H), 3.84 (s, 2H), 3.74 (s, 4H), 2.66 (s, 4H). ¹³C NMR (75 MHz, CDCl_3) δ : 182.5, 178.4, 167.2, 135.1, 131.9, 130.9, 130.6, 130.4, 128.3, 125.4, 122.8, 67.6, 54.2, 52.8. IR (ν , cm^{-1}): 3474, 3415, 2926, 2361, 2342, 1690, 1402, 1108, 784. ESI-HRMS m/z [$\text{M}+\text{H}$]⁺ calculated for $\text{C}_{16}\text{H}_{15}\text{N}_2\text{O}_4$: 299.1026, found: 299.1033.

4.1.6.3. 2-(((2-Methoxyphenyl)amino)methyl)naphtho[2,1-d]oxazole-4,5-dione (3e). Yield: 41%. Dark red solid, mp 181–183 °C. ¹H NMR (300 MHz, CDCl_3) δ : 8.16 (d, J = 7.7 Hz, 1H), 7.74–7.71 (m, 2H), 7.60 (t, J = 6.9 Hz, 1H), 6.93–6.89 (m, 4H), 4.73 (s, 2H), 3.92 (s, 3H). IR (ν , cm^{-1}): 3418, 2924, 2850, 1672, 1604, 1591, 1272, 1218, 1037, 910, 771, 473. ESI-HRMS m/z [$\text{M}+\text{H}$]⁺ calculated for $\text{C}_{19}\text{H}_{15}\text{N}_2\text{O}_4$: 335.1026, found: 335.1031.

4.1.6.4. 2-(((3-Methoxyphenyl)amino)methyl)naphtho[2,1-d]oxazole-4,5-dione (3f). Yield: 34%. Dark red solid, mp 193–194 °C. ¹H NMR (300 MHz, CDCl_3) δ : 8.15 (d, J = 7.8 Hz, 1H), 7.71–7.68 (m, 2H), 7.56 (t, J = 5.3 Hz, 1H), 7.13 (t, J = 7.9 Hz, 1H), 6.36 (d, J = 8.2 Hz, 2H), 6.30 (s, 1H), 4.60 (s, 2H), 3.78 (s, 3H). IR (ν , cm^{-1}): 3415, 2922, 2851, 1669, 1602, 1590, 1262, 1213, 1039, 910, 771, 469. ESI-HRMS m/z [$\text{M}+\text{H}$]⁺ calculated for $\text{C}_{19}\text{H}_{15}\text{N}_2\text{O}_4$: 335.1026, found: 335.1029.

4.1.6.5. 2-(((4-Methoxyphenyl)amino)methyl)naphtho[2,1-d]oxazole-4,5-dione (3g). Yield: 30%. Dark red solid, mp 178–180 °C. ¹H NMR (300 MHz, CDCl_3) δ : 8.14 (d, J = 7.8 Hz, 1H), 7.68 (s, 2H), 7.57–7.55 (m, 1H), 6.79–6.73 (m, 4H), 4.57 (s, 2H), 3.74 (s, 3H). ¹³C NMR (75 MHz, CDCl_3) δ : 181.9, 179.2, 163.9, 152.5, 151.3, 139.8, 135.1, 130.9, 130.7, 129.1, 126.2, 125.2, 122.6, 114.5, 114.2, 55.2, 41.9. IR (ν , cm^{-1}): 3414, 2360, 2341, 1662, 1618, 1512, 1238, 1050, 911, 474. ESI-HRMS m/z [$\text{M}+\text{H}$]⁺ calculated for $\text{C}_{19}\text{H}_{15}\text{N}_2\text{O}_4$: 335.1026, found: 335.1031.

4.1.6.6. 2-(((4-Methoxyphenyl)amino)methyl)naphtho[2,1-d]oxazole-4,5-dione (3h). Yield: 35%. Red solid, mp 151–153 °C. ¹H NMR (300 MHz, DMSO) δ : 7.96 (d, J = 8.6 Hz, 1H), 7.56 (t, J = 7.2 Hz, 1H), 7.67–7.59 (m, 2H), 6.90 (d, J = 8.2 Hz, 2H), 6.60 (d, J = 8.2 Hz, 2H), 4.53 (d, J = 6.3 Hz, 2H), 2.12 (s, 3H). IR (ν , cm^{-1}): 3414, 2919, 1678, 1638, 1521, 910, 468. ESI-HRMS m/z [$\text{M}+\text{H}$]⁺ calculated for $\text{C}_{19}\text{H}_{15}\text{N}_2\text{O}_3$: 319.1077, found: 319.1083.

4.1.6.7. 2-(((4-Chlorophenyl)amino)methyl)naphtho[2,1-d]oxazole-4,5-dione (3i). Yield: 38%. Red solid, mp 175–177 °C. ¹H NMR (300 MHz, DMSO) δ : 7.96 (d, J = 7.7 Hz, 1H), 7.56 (t, J = 6.7 Hz, 1H), 7.67–7.59 (m, 2H), 7.11 (d, J = 8.2 Hz, 2H), 6.70 (d, J = 8.6 Hz, 2H), 4.57 (d, J = 6.1 Hz, 2H). IR (ν , cm^{-1}): 3415, 3316, 2366, 1669, 1618, 1420, 1216, 1048, 912. ESI-HRMS m/z [$\text{M}+\text{H}$]⁺ calculated for $\text{C}_{18}\text{H}_{12}\text{ClN}_2\text{O}_3$: 339.0531, found: 339.0532.

4.1.6.8. 2-(((3-Fluorophenyl)amino)methyl)naphtho[2,1-d]oxazole-4,5-dione (3j). Yield: 35%. Red solid, mp 182–184 °C. ¹H NMR (300 MHz, DMSO) δ : 7.97 (d, J = 7.7 Hz, 1H), 7.62 (t, J = 6.4 Hz, 1H), 7.67–7.57 (m, 2H), 7.11–7.05 (m, 1H), 6.79 (t, J = 6.6 Hz, 1H), 6.52 (d, J = 7.8 Hz, 1H), 6.35 (t, J = 9.5 Hz, 1H), 4.60 (d, J = 6.3 Hz, 2H). IR (ν , cm^{-1}): 3415, 3326, 2923, 2361, 2342, 1671, 1617, 1212, 1159, 910, 771, 689, 486. ESI-HRMS m/z [$\text{M}+\text{Na}$]⁺ calculated for $\text{C}_{18}\text{H}_{12}\text{FN}_2\text{O}_3$: 323.0826, found: 323.0817.

4.1.6.9. 2-((4-Benzylpiperazin-1-yl)methyl)naphtho[2,1-d]oxazole-4,5-dione (3k). Yield: 42%. Red solid, mp 168–169 °C. ¹H NMR (300 MHz, CDCl₃) δ: 8.16 (d, *J* = 7.5 Hz, 1H), 7.73 (d, *J* = 8.8 Hz, 2H), 7.58 (t, *J* = 8.8 Hz, 1H), 7.44–7.28 (m, 5H), 3.87 (s, 2H), 3.54 (s, 2H), 2.70–2.54 (m, 8H). ¹³C NMR (75 MHz, CDCl₃) δ: 179.1, 171.8, 162.5, 158.9, 137.3, 135.1, 133.4, 130.9, 130.6, 128.8, 128.7, 127.7, 126.6, 125.3, 122.8, 62.4, 53.8, 52.4, 52.2. IR (ν, cm⁻¹): 3415, 2919, 2812, 1683, 1587, 1453, 1122, 697, 465. ESI-HRMS *m/z* [M+H]⁺ calculated for C₂₃H₂₂N₃O₃: 388.1656, found: 388.1656.

4.1.6.10. 2-((4-Phenylpiperazin-1-yl)methyl)naphtho[2,1-d]oxazole-4,5-dione (3l). Yield: 34%. Red solid, mp 174–176 °C. ¹H NMR (300 MHz, CDCl₃) δ: 8.06–7.98 (m, 1H), 7.90–7.82 (m, 2H), 7.64 (t, *J* = 6.7 Hz, 1H), 7.52 (t, *J* = 7.0 Hz, 1H), 7.33–7.23 (m, 2H), 7.01 (d, *J* = 8.0 Hz, 1H), 6.83 (t, *J* = 6.9 Hz, 1H), 4.98 (s, 2H), 3.55–3.35 (m, 8H). ¹³C NMR (75 MHz, CDCl₃) δ: 180.3, 177.8, 167.0, 150.5, 141.0, 133.0, 132.9, 131.3, 130.4, 129.3, 128.8, 127.8, 126.2, 120.2, 116.1, 54.1, 49.9, 49.2. IR (ν, cm⁻¹): 3415, 1736, 1637, 1584, 1497, 1228, 1017. ESI-HRMS *m/z* [M+H]⁺ calculated for C₂₂H₂₀N₃O₃: 374.1499, found: 374.1499.

4.2. Biology

4.2.1. In vitro NQO1 assay

ortho-Naphthoquinones (0.1–50 μmol·L⁻¹) were monitored as NQO1 substrates using an NADPH recycling assay and recombinant NQO1 (DT-diaphorase, EC 1.6.5.5, human recombinant, Sigma), in which NADPH oxidation to NADP⁺ was monitored by absorbance (A₃₄₀ nm) on a Varioskan Flash (Thermo, Waltham, MA). Compounds in DMSO stock (2 μL) were added to a 96 plate. NADPH (400 μmol·L⁻¹) and NQO1 (1.4 μg/mL) in 50 mmol·L⁻¹ potassium phosphate buffer (pH = 7.4) were added to each well (198 μL). Once the 96-well plate was filled with the assay solutions, except the NADPH solution, it was placed into the instrument and left to sit for 3 min before starting the measurements. The enzyme reaction was initiated by automated dispensing of the NADPH solution into the wells, and data was recorded at 2 s intervals for 5 min at room temperature (22–25 °C). The linear portion of the absorbance vs time graphs (the first 20 s to 1 min) were fitted, and the slopes were calculated (velocity). NADPH oxidation rates were compared with reactions lacking compound. Initial velocities were calculated and data expressed as μmol NADPH oxidized/min/μmol protein. All reactions were carried out at least in triplicate.

4.2.2. Physicochemical properties

At the neutral solution, the aqueous solubility and Log_{D7.4} were determined on a Gemini Profiler instrument (pION) by the 'gold-standard' Avdeef–Bucher potentiometric titration method.²⁵ Under acidic condition,²⁶ the compounds were treated with the diluted hydrochloric acid buffer solution, then shaken at 25 °C for 8 h. A visual inspection was made as to whether the test substance was fully in solution or not. Compounds which were not completely soluble at 500 μg/mL were diluted to 100 μg/mL and the process repeated until the compound dissolved.

4.2.3. Molecular modeling

A docking study was performed using the crystal structure of the human NQO1 complex with dicoumarol (PDB code: 2F1O and resolution 2.75 Å) and the structure was edited according to provide a monomer of the protein and protonated using GOLD 5.1. The ligand was then removed to leave the receptor complex, which was used for the subsequent docking studies. For preparation of ligand structures, the selected analogs were energy minimized using MOE 2013.08 with an MMFF94x forcefield using gas phase calculations and a cutoff of 0.01. Charges were then fixed using

an MMFF94 forcefield. For computational docking, GOLD 5.1 software was used in combination with ChemScore scoring function. The active site was defined as being any volume within 8 Å of the scaffold of dicoumarol in its crystal pose in 2F1O. The number of genetic algorithm (GA) run was set to 10, and scoring of the docked poses was performed with the ChemScore scoring function. Each GOLD run was saved and the strongest scoring binding pose of each ligand (subject to a rmsd default distance threshold of 1.5 Å) was compared to that of the reference ligand position observed in the crystal structure. The best output poses of the ligands generated were analyzed on the basis of ChemScore, feasibility of hydride transfer process, and H-bonding to the enzyme. The best poses were visualized with MOE 2013.08.²⁴

4.2.4. Cell lines and culture

Human cell lines (NQO1-rich), NCI-H596 and human normal liver cell LO2 were obtained from the American Type Culture Collection (ATCC, USA). All of these cells were cultured in Roswell Park Memorial Institute (RPMI) 1640 medium, supplemented with 10% fetal bovine serum (FBS) at 37 °C and 5% CO₂.

4.2.5. Cell viability assay

Growth inhibition was determined by the MTT colorimetric assay. Cells were plated in 96-well plates at a density of 10,000 cells/mL and allowed to attach overnight (16 h). Cells were then exposed to various concentrations of test compounds in triplicate for 2 h, removed, and replaced with fresh medium, and the plates were incubated at 37 °C under a humidified atmosphere containing 5% CO₂ for 72 h. MTT (50 μg) was added and the cells were incubated for another 4 h. Medium/MTT solutions were removed carefully by aspiration, the MTT formazan crystals were dissolved in 100 μL of DMSO, and absorbance was determined on a plate reader at 560 nm. When investigating the effect of dicoumarol, cells were cotreated with vehicle or 25 μmol·L⁻¹ dicoumarol and compound **3k** for 2 h with at least three technical replicates. IC₅₀ values (concentration at which cell survival equals 50% of control) were determined from semilog plots of percent of control versus concentration.

4.2.6. Superoxide generation assays

The reduction of *ortho*-naphthoquinones and the resulting was monitored by a spectrophotometric assay in which the rate of reduction of cytochrome *c* was quantified at 550 nm. Briefly, the assay mixture contained cytochrome *c* (30 μmol·L⁻¹), reduced nicotinamide adenine dinucleotide (NADPH; 0.2 mmol·L⁻¹), recombinant human NQO1 (0.1–3.0 μg/mL) (DT-diaphorase, EC 1.6.5.5, human recombinant, Sigma), and naphthoquinones (25 μmol·L⁻¹) in a final volume of 1 mL of Tris–HCl (25 mmol·L⁻¹, pH 7.4) containing 0.7 mg/mL bovine serum albumin (BSA) and 0.1% Tween-20. Reactions were carried out at room temperature and started by the addition of NADPH. Rates of reduction were calculated from the initial linear part of the reaction curve (0–30 s), and results were expressed in terms of micromoles of cytochrome *c* reduced per minute per milligram of NQO1 by use of a molar extinction coefficient of 21.1 mM⁻¹·cm⁻¹ for cytochrome *c*. All reactions were carried out at least in triplicate.

4.2.7. In vivo antitumor efficacy

Log-phase A549 cells (5 × 10⁶) were injected into the flanks of athymic nude mice (aged 7–8 weeks). Tumor sizes were regularly measured using calipers, and volumes were calculated using the following formula: volume (mm³) = *a* × *b*²/2, *a* and *b* represent the length and width. Animals were randomized into four groups (5 mice/group) when the average tumor size reached 100 mm³ for the following treatments: group 1, vehicle; group 2, **3k** (15 mg/kg); group 3, **3k** (30 mg/kg), and group 4, β-lap (ARQ501,

30 mg/kg) injection. Compound **3k** was dosed diluted in hydrochloric acid buffer at pH = 3. ARQ501 was dosed in normal saline. All agents were administered every other day for three weeks through tail vein injection. Tumor sizes were monitored and measured every day. After three weeks, mice were euthanized and the average tumor wet weights were calculated.

Acknowledgements

We are thankful for the financial support of the National Natural Science Foundation of China (No. 81302636), the Natural Science Foundation of Jiangsu Province of China (No. BK20130656), National Found for Fostering Talents of Basic Science (NFFTS) (No. J1030830), and the Priority Academic Program Development of Jiangsu Higher Education Institutions (PAPD), the Research Innovation Program for College Graduates of Jiangsu Province of 2015 (Grant No. KYLX15_0634).

Supplementary data

Supplementary data associated with this article can be found, in the online version, at <http://dx.doi.org/10.1016/j.bmc.2016.01.024>.

References and notes

- Kongkathip, N.; Kongkathip, B.; Siripong, P.; Sangma, C.; Luangkamin, S.; Niyomdech, M.; Pattanapa, S.; Piyaviriyagul, S.; Kongsaree, P. *Bioorg. Med. Chem.* **2003**, *11*, 3179.
- Sasaki, J.; Sano, K.; Hagimori, M.; Yoshikawa, M.; Maeda, M.; Mukai, T. *Bioorg. Med. Chem.* **2014**, *22*, 6039.
- Scott, K. A.; Barnes, J.; Whitehead, R. C.; Stratford, I. J.; Nolan, K. A. *Biochem. Pharmacol.* **2011**, *81*, 355.
- Huang, X.; Dong, Y.; Bey, E. A.; Kilgore, J. A.; Bair, J. S.; Li, L. S.; Patel, M.; Parkinson, E. I.; Wang, Y.; Williams, N. S.; Gao, J.; Hergenrother, P. J.; Boothman, D. A. *Cancer Res.* **2012**, *72*, 3038.
- Raj, L.; Ide, T.; Gurkar, A. U.; Foley, M.; Schenone, M.; Li, X.; Tolliday, N. J.; Golub, T. R.; Carr, S. A.; Shamji, A. F.; Stern, A. M.; Mandinova, A.; Schreiber, S. L.; Lee, S. W. *Nature* **2011**, *475*, 231.
- Pathania, D.; Sechi, M.; Palomba, M.; Sanna, V.; Berrettini, F.; Sias, A.; Taheri, L.; Neamati, N. *BBA-Gen Subj.* **2014**, *1840*, 332.
- Muller, M. *Free Radial Biol. Med.* **2009**, *47*, 84.
- Gellis, A.; Kovacic, H.; Boufatah, N.; Vanelle, P. *Eur. J. Med. Chem.* **2008**, *43*, 1858.
- Liu, F.; Yu, G.; Wang, G.; Liu, H.; Wu, X.; Wang, Q.; Liu, M.; Liao, K.; Wu, M.; Cheng, X.; Hao, H. *PLoS One* **2012**, *7*, e42138.
- Bian, J.; Deng, B.; Xu, L.; Xu, X.; Wang, N.; Hu, T.; Yao, Z.; Du, J.; Yang, L.; Sun, H.; Zhang, X.; You, Q. *Eur. J. Med. Chem.* **2014**, *82*, 56.
- Bian, J.; Xu, L.; Deng, B.; Qian, X.; Fan, J.; Yang, X.; Liu, F.; Xu, X.; Guo, X.; Li, X.; Sun, H.; You, Q.; Zhang, X. *Bioorg. Med. Chem. Lett.* **2015**, *25*, 1244.
- Bian, J.; Deng, B.; Zhang, X.; Hu, T.; Wang, N.; Wang, W.; Pei, H.; Xu, Y.; Chu, H.; Li, X.; Sun, H.; You, Q. *Tetrahedron Lett.* **2014**, *55*, 1475.
- Ma, X.; Huang, X.; Moore, Z.; Huang, G.; Kilgore, J. A.; Wang, Y.; Hammer, S.; Williams, N. S.; Boothman, D. A.; Gao, J. *J. Controlled Release* **2015**, *200*, 201.
- Naujorks, A. A.; da Silva, A. O.; Lopes, R. da S.; Albuquerque, S. de; Beatriz, A.; Marques, M. R.; de Lima, D. P. *Org. Biomol. Chem.* **2015**, *13*, 428.
- Nasongkla, N.; Wiedmann, A.; Bruening, A.; Beman, M.; Ray, D.; Bornmann, W.; Boothman, D.; Gao, J. *Pharm. Res.* **2003**, *20*, 1626.
- Ma, X.; Moore, Z. R.; Huang, G.; Huang, X.; Boothman, D. A.; Gao, J. *J Drug Target* **2015**, *23*, 672.
- Parkinson, E. I.; Bair, J. S.; Cismesia, M.; Hergenrother, P. J. *ACS Chem. Biol.* **2013**, *8*, 2173.
- Faig, M.; Bianchet, M. A.; Winski, S.; Hargreaves, R.; Moody, C. J.; Hudnott, A. R.; Amzel, L. M. *Structure* **2001**, *9*, 659.
- Bianchet, M. A.; Faig, M.; Amzel, L. M. *Methods Enzymol.* **2004**, *382*, 144.
- Nolan, K. A.; Doncaster, J. R.; Dunstan, M. S.; Scott, K. A.; Frenkel, A. D.; Siegel, D.; Bryce, R. A. *J. Med. Chem.* **2009**, *52*, 7142.
- Faig, M.; Bianchet, M. A.; Talalay, P.; Chen, S.; Winski, S.; Ross, D.; Amzel, L. M. *Proc. Natl. Acad. Sci. U.S.A.* **2000**, *97*, 3177.
- Mendoza, M. F.; Hollabaugh, N. M.; Hettiarachchi, S. U.; McCarley, R. L. *Biochemistry* **2012**, *51*, 8014.
- Tarpey, M. M.; Wink, D. A.; Grisham, M. B. *Integr. Comp. Physiol.* **2004**, *286*, R431.
- Version 2013.08, *Molecular Operating Environment*; Chemical Computing Group: Montreal, QC, 2013.
- Xu, L.; Zhu, J.; Xu, X.; Zhu, J.; Li, L.; Xi, M.; Jiang, Z.; Zhang, M.; Liu, F.; Li, M.; Bao, Q.; Li, Q.; Zhang, C.; Wei, J.; Zhang, X.; Zhang, L.; You, Q.; Sun, H. *J. Med. Chem.* **2015**, *58*, 5419.
- Woodhead, A. J.; Angove, H.; Carr, M. G.; Chessari, G.; Congreve, M.; Coyle, J. E.; Cosme, J.; Graham, B.; Day, P. J.; Downham, R.; Fazal, L.; Feltell, R.; Figueroa, E.; Frederickson, M.; Lewis, J.; McMennamin, R.; Murray, C. W.; O'Brien, M. A.; Parra, L.; Patel, S.; Phillips, T.; Rees, D. C.; Rich, S.; Smith, D. M.; Trewartha, G.; Vinkovic, M.; Williams, B.; Woolford, A. J. *J. Med. Chem.* **2010**, *53*, 5956.